

# Toroidal flow stabilization of disruptive high $\beta$ tokamaks

Robert G. Kleva and Parvez N. Guzdar

*Institute for Plasma Research, University of Maryland, College Park, Maryland 20742-3511*

(Received 4 February 2002; accepted 27 February 2002)

Disruptive high  $\beta$  tokamak plasmas can be stabilized by the addition of a sheared toroidal flow. Nonlinear simulations demonstrate that confinement in flow-free high  $\beta$  tokamaks is rapidly destroyed by growing fingers of hot plasma that jet out from the center of the discharge to the wall. The added toroidal flow eliminates the growing fingers, maintaining confinement. As  $\beta$  increases further, the toroidal flow becomes less effective at maintaining a stable plasma. But a sound speed toroidal flow increases the critical value of  $\beta$  below which confinement is maintained without disruptions. © 2002 American Institute of Physics. [DOI: 10.1063/1.1475682]

## I. INTRODUCTION

The fusion of light nuclei in a magnetically confined tokamak plasma provides a potentially unlimited source of energy. Since the rate at which the nuclei fuse is proportional to the square of the number density of nuclei, it is desirable to operate a fusion reactor at high density. However, the amount of thermal energy that can be stably confined at the center of tokamak discharges is limited by disruptions. When the ratio  $\beta$  of the plasma thermal energy to the magnetic field energy exceeds a critical value  $\beta_{\text{crit}}$ , then there is an abrupt, catastrophic loss of confinement on a time scale of the order of 100  $\mu\text{s}$ .<sup>1</sup>

Our magnetohydrodynamic (MHD) simulations of tokamaks<sup>2</sup> have demonstrated that tokamaks at high  $\beta$  are unstable to a spectrum of ballooning modes with toroidal mode number  $n$  that grow on the pressure gradient on the large  $R$  side of the magnetic axis, where  $R$  is the major radial coordinate in toroidal geometry. Nonlinearly, the ballooning mode convection cells generate ridges of hot plasma and valleys of cold plasma that extend toroidally along the outside of the torus.<sup>3,4</sup> When projected onto a two-dimensional plane, these ridges and valleys have the appearance of fingers. The rate at which these fingers grow and transport energy is proportional to the magnitude of  $\beta$ . At lower  $\beta$  the fingers grow more slowly and are halted nonlinearly by a self-generated axisymmetric flow,<sup>3</sup> and confinement is maintained. But at higher  $\beta$  the fingers grow too rapidly to be affected by the axisymmetric flow, and the fingers of hot plasma rapidly convect across the magnetic field lines from the center of the discharge to the wall, thereby destroying confinement.<sup>2-4</sup> Simultaneously, fingers of cold edge plasma are injected across the magnetic field lines into the center of the discharge. Importantly, the rate at which energy is transported to the wall by the fingers is independent of the magnitude of the resistivity  $\eta$ .<sup>4</sup> As  $\eta$  is reduced in magnitude, the number of fingers increases, with the width of each individual finger becoming more narrow. But these more numerous, narrower fingers at lower  $\eta$  transport energy at the same rate as the wider fingers at higher  $\eta$ . Because of the increasingly fine scale fingers generated as  $\eta$  is decreased, the time scale for diffusion of the magnetic field across the fingers is

independent of the magnitude of the resistivity.<sup>4</sup> As a consequence, the magnetic field lines are decoupled from the plasma fingers (not “frozen-in”) even as  $\eta$  approaches zero. The limit of resistive MHD as  $\eta \rightarrow 0$  is not the same as ideal MHD with  $\eta = 0$ .

Because of the disastrous consequences that these growing fingers have on tokamak energy confinement at high  $\beta$ , it is important to investigate potential mechanisms that may ameliorate their effect. Sheared flows are one such possible stabilizing mechanism. Sheared toroidal flows have been found to have a stabilizing influence on the local linear ideal MHD stability of ballooning modes with toroidal mode number  $n \rightarrow \infty$ .<sup>5-8</sup> Since the nonlinear ridges and fingers in our toroidal simulations balloon on the pressure gradient on the large  $R$  side of the torus, a sheared toroidal flow may act to oppose their growth.

In this paper we investigate the effect of a sheared toroidal flow on the nonlinear evolution of the fingers that destroy confinement at high  $\beta$ . Our nonlinear MHD simulations of tokamaks with toroidal flows demonstrate that (1) sheared toroidal flows have a stabilizing effect on high  $\beta$  tokamaks. The flow can stabilize an otherwise disruptive plasma, maintaining confinement. (2) Sound speed toroidal flows increase the critical value of  $\beta$  below which confinement is maintained without disruptions. (3) For slow flows the fingers are still unstable. However, they grow much more slowly than in a flow-free plasma. The fingers no longer balloon out toward the wall at large  $R$ , but instead rotate about the magnetic axis. Energy slowly spirals out to the wall on a much longer time scale than in a flow-free plasma. (4) As  $\beta$  increases further, the fingers become more difficult to control. The Mach number of the toroidal flow must be increased as  $\beta$  is increased in order to maintain confinement. (5) As the magnitude of the transport coefficients (resistivity  $\eta$  and viscosity  $\mu$ ) is decreased, the toroidal flow becomes more stabilizing. The toroidal flow is more effective at maintaining confinement when the Lundquist number  $S$  is large.

The rest of this paper is organized as follows. Equilibrium in a torus with toroidal flows is considered in Sec. II. The equations used in the simulations are presented and the numerical procedure used to solve these equations is outlined. As a baseline, in Sec. III we present the results of

simulations of flow-free high  $\beta$  tokamaks. The effect of a toroidal flow on the nonlinear stability of high  $\beta$  tokamak plasmas is presented in Sec. IV. The effect of varying the Mach number  $M$ , the plasma pressure  $\beta$ , and the transport coefficients is investigated. We discuss our results in Sec. V.

## II. TOROIDAL EQUILIBRIA WITH TOROIDAL FLOWS

Our numerical simulations of nonlinear stability in tokamaks with toroidal flows are based on the resistive MHD equations for the magnetic field  $\mathbf{B}$ , the mass velocity  $\mathbf{V}$ , the temperature  $T$ , and the mass density  $\rho_m$ :

$$\partial\mathbf{B}/\partial t = \nabla \times (\mathbf{V} \times \mathbf{B}) + \eta \nabla^2 \mathbf{B} + \nabla \times \mathbf{E}_0, \quad (1)$$

$$\partial\mathbf{U}/\partial t + \nabla \cdot (\mathbf{V}\mathbf{U}) = \mathbf{J} \times \mathbf{B} - \nabla P + \mu \nabla^2 \mathbf{U} + S_\phi \hat{\phi}, \quad (2)$$

$$\partial T/\partial t + \mathbf{V} \cdot \nabla T - \nabla_{\parallel} \kappa_{\parallel} \nabla_{\parallel} T = 0, \quad (3)$$

$$\partial \rho_m / \partial t + \nabla \cdot \mathbf{U} - D \nabla^2 \rho_m = S_{\rho_m}, \quad (4)$$

where the parallel gradient  $\nabla_{\parallel} = \hat{\mathbf{b}} \cdot \nabla$  with  $\hat{\mathbf{b}} = \mathbf{B}/|\mathbf{B}|$ , the momentum density  $\mathbf{U} = \rho_m \mathbf{V}$ , the pressure  $P = \rho_m T$ , and the current  $\mathbf{J} = \nabla \times \mathbf{B}$ , for a plasma with resistivity  $\eta$ , viscosity  $\mu$ , parallel thermal conductivity  $\kappa_{\parallel}$ , and diffusion coefficient  $D$ . The external electric field  $\mathbf{E}_0$  maintains the poloidal magnetic field against resistive diffusion, and the sources  $S_\phi$  and  $S_{\rho_m}$  maintain the toroidal flow and the mass density against transport losses. Equations (1)–(4) are solved in toroidal geometry  $(R, \phi, z)$ , where  $R$  is the major radial coordinate of the torus,  $\phi$  is the toroidal angle, and  $z$  is the vertical distance along the axis of the torus. The equations are given in normalized units<sup>9</sup> in which distances in  $R$  and  $z$  are normalized to a scale length  $a$ , the velocity  $\mathbf{V}$  is normalized to the Alfvén speed  $v_A$ , the time  $t$  is normalized to the Alfvén time  $\tau_A \equiv a/v_A$ , the resistivity  $\eta = S^{-1}$  where the Lundquist number  $S \equiv \tau_r/\tau_A$  is the ratio of the resistive diffusion time  $\tau_r$  to the Alfvén time, and the sound speed  $c_s = \sqrt{T}$ . The magnetic field in toroidal geometry can be written in the form

$$\mathbf{B} = \nabla \psi \times \hat{\phi}/R + B_\phi \hat{\phi}, \quad (5)$$

where  $\psi$  is the poloidal magnetic flux and  $\hat{\phi}$  is a unit vector in the  $\phi$  direction.

Axisymmetric equilibria, independent of the toroidal angle  $\phi$ , are obtained from Eqs. (1)–(4) by neglecting the time derivatives. In equilibrium, the net force in the momentum equation (2) must be zero,

$$-\nabla P + \mathbf{J} \times \mathbf{B} + \hat{R} \rho_m V_\phi^2/R = 0, \quad (6)$$

where  $V_\phi$  is the equilibrium toroidal flow velocity and  $\hat{R}$  is a unit vector in the  $R$  direction. In addition to the usual force caused by the pressure gradient and the Lorentz  $\mathbf{J} \times \mathbf{B}$  force, there is an additional centrifugal force outward in the major radius because of the toroidal flow.

The rapid transport of energy along the magnetic field lines forces the equilibrium temperature to be uniform along the equilibrium magnetic field lines:  $\mathbf{B} \cdot \nabla T = 0$ . With expression (5) for the magnetic field, it is easy to show that this condition is satisfied if the temperature is a function  $T(\psi)$  of the flux  $\psi$ .

The toroidal flow  $V_\phi$  will alter the equilibrium magnetic field unless the flow satisfies the equation  $\nabla \times (V_\phi \hat{\phi} \times \mathbf{B}) = 0$ . With expression (5) for the magnetic field, it is straightforward to show that the equilibrium magnetic field will not be altered by the flow if  $V_\phi$  is given by the product of the major radius  $R$  and an arbitrary function  $f(\psi)$  of the flux  $\psi$ . It is convenient to take  $f(\psi)$  to be proportional to the sound speed  $c_s = \sqrt{T(\psi)}$ . Then we write  $V_\phi$  in the form

$$V_\phi = M \frac{R}{R_{\text{axis}}} \sqrt{T(\psi)}, \quad (7)$$

where  $R_{\text{axis}}$  is the position of the magnetic axis in major radius. The ratio of the toroidal flow velocity to the sound speed is given by the Mach number  $M$ ,

$$V_\phi/c_s = M \frac{R}{R_{\text{axis}}}. \quad (8)$$

The mass density  $\rho_m$  is determined by the force balance equation (6) together with expression (7) for  $V_\phi$ . Let us take  $\rho_m$  to be a function of the major radius  $R$  so that the pressure  $P(R, \psi) = \rho_m(R)T(\psi)$ . Then the component of the force balance equation (6) parallel to the magnetic field can be written as

$$\frac{d}{dR} \rho_m = \rho_m M^2 R / R_{\text{axis}}^2. \quad (9)$$

Equation (9) can be integrated to give the equilibrium mass density

$$\rho_m = e^{(1/2) M^2 [(R/R_{\text{axis}})^2 - 1]}. \quad (10)$$

By specifying the flux  $\psi$ , the temperature  $T(\psi)$  as a function of  $\psi$ , and  $V_\phi$  and  $\rho_m$  as a function of the Mach number  $M$  through Eqs. (7) and (10), respectively, we ensure that the component of the force parallel to the magnetic field is zero in equilibrium. However, the component of the force perpendicular to the magnetic field is not, in general, zero. We obtain an axisymmetric equilibrium dynamically by solving the two-dimensional component of the MHD equations for the magnetic field (1) and the momentum (2) in the poloidal plane  $(R, z)$ . The net force on the plasma perpendicular to the magnetic field generates a mass flow which alters the magnetic field and, hence, the flux  $\psi$ . The temperature is then determined through the functional form  $T(\psi)$ , and the toroidal flow and the mass density are determined from Eqs. (7) and (10), respectively. With the resistivity  $\eta = 0$ , but with a nonzero viscosity  $\mu$ , the system relaxes into an equilibrium in which the force balance equation (6) is satisfied. The small residual flow is damped away by the viscosity.

An example of an equilibrium with a sound speed toroidal flow (Mach number  $M = 1$ ) is shown in Fig. 1. Figure 1(a) is a plot of the toroidal flow  $V_\phi$  (solid line) and the pressure  $P$  (dashed line) as a function of the major radius  $R$  through the midplane ( $z = 0$ ) of a torus, for a plasma with  $\beta = 2P_0/B_{\phi 0}^2 = 2\%$ , where  $P_0$  is the pressure at the magnetic axis and  $B_{\phi 0}$  is the toroidal magnetic field at the magnetic axis. The safety factor  $q$  in this equilibrium increases monotonically from 1.1 at the magnetic axis to 3.3 at the wall.

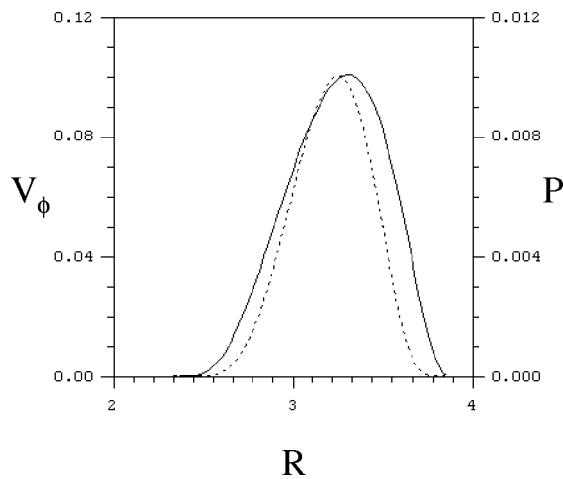


FIG. 1. Equilibrium with a sound speed toroidal flow. The toroidal flow  $V_\phi$  (solid line) and the pressure  $P$  (dashed line) are plotted as a function of the major radius  $R$  through the midplane ( $z=0$ ) of a torus for a plasma with  $\beta=2\%$ .

The nonlinear equations are solved on a Cartesian grid in  $R$ ,  $\phi$ , and  $z$ . Spatial derivatives are evaluated to fourth order in the grid spacing  $\Delta$  (Ref. 10), while time stepping is second order accurate in the time step  $\Delta t$  with a leap frog trapezoidal scheme.<sup>11</sup>

### III. DISRUPTIONS AT HIGH $\beta$

The nonlinear evolution of a flow-free ( $M=0$ ) tokamak plasma at high  $\beta$  is illustrated by the simulation results shown in Fig. 2. This figure contains a series of plots that illustrate the temporal evolution of the temperature in the poloidal plane ( $R, z$ ) at toroidal angle  $\phi=0$ . The hottest plasma is located in the red region. The plasma becomes progressively cooler through the orange, yellow, green, and blue regions, with the coldest plasma located in the violet region. The boundary of the plasma lies at the inner edge of the light blue area located at the edge of each plot. Two different simulations are shown in Fig. 2. These two simulations differ only in the temperature of the equilibrium; all other parameters are identical. The transport coefficients  $\eta = \mu = D = 3 \times 10^{-4}$ , and the parallel thermal conduction  $\kappa_{\parallel} = 1$ . The series of plots on the left-hand side of Fig. 2 show the temporal evolution of a plasma with  $\beta=1\%$ , while the nonlinear evolution of a plasma with  $\beta=2\%$  is given by the plots on the right-hand side.

In each case, an identical, small, three-dimensional perturbation was applied to the tokamak equilibrium at  $t=0$ . In both cases the plasma is unstable. Convection cells develop and the plasma flow in these cells transports the hot central plasma to the wall in ridges that extend toroidally around the outside of the torus. The two-dimensional projection of these ridges onto the poloidal plane has the appearance of fingers. When  $\beta=1\%$ , these fingers become sizable by  $t=600\tau_A$ . The hot plasma fingers continue to rapidly grow towards the wall at large  $R$  at  $t=900\tau_A$ , destroying confinement. Simultaneously fingers of cold edge plasma grow inward towards the center of the plasma column.

As the equilibrium  $\beta$  increases, confinement is destroyed in the same manner, although even more rapidly. When  $\beta=2\%$ , the fingers become sizable by  $t=250\tau_A$ , and the fingers continue their rapid convection nearly reaching the wall at large  $R$  by  $t=400\tau_A$ . As a result of doubling the temperature, confinement has been destroyed in about half the time.

## IV. CONFINEMENT WITH TOROIDAL FLOWS

### A. Mach number $M$

Consider now the effect of a sheared toroidal flow on tokamak confinement at high  $\beta$ . The plots in Fig. 3 illustrate the effect of toroidal flows on the nonlinear stability of a  $\beta=1\%$  tokamak plasma. The simulations shown in Fig. 3 are identical to the  $\beta=1\%$  simulation shown on the left-hand side of Fig. 2, with the same initial perturbation at  $t=0$ , except for the addition of a toroidal flow with Mach number  $M$  to the equilibrium.

When the speed of the toroidal flow rises to 30% of the sound speed ( $M=0.3$ ), the plasma is still unstable but the perturbation grows more slowly. The plots on the left-hand side of Fig. 3 show the nonlinear evolution of a  $\beta=1\%$  tokamak plasma with a toroidal flow of Mach number  $M=0.3$ . Structures with a finger-like appearance grow, but the fingers no longer balloon out to the wall at large  $R$  as in the flow-free case. Instead, the fingers are more uniformly distributed in poloidal angle. These fingers slowly rotate in the poloidal plane about the magnetic axis. As the fingers rotate, the thermal energy slowly spirals out from the center towards the wall over a time scale of several thousand Alfvén times. This transport of energy is much slower than the rapid disruptive loss of confinement seen in the flow-free simulation.

When the toroidal flow speed increases to the sound speed  $M=1$ , then confinement is maintained by the flow. The plots on the right-hand side of Fig. 3 show the effect of a sound speed toroidal flow on nonlinear stability when  $\beta=1\%$ . The hot plasma remains confined at the center of the poloidal cross-section, away from the wall. The sheared sonic toroidal flow has eliminated the growing fingers that had caused a rapid loss of thermal energy in the flow-free plasma.

### B. Plasma pressure $\beta$

As  $\beta$  increases in a flow-free tokamak plasma, confinement is destroyed ever more rapidly by the growing plasma fingers (Fig. 2). The plots on the left-hand side of Fig. 4 show the effect of a sound speed  $M=1$  toroidal flow on nonlinear stability when  $\beta=2\%$ . Thin rotating fingers slowly grow, resulting in a slow spiralling of thermal energy from the center out toward the wall over a time scale of several thousand Alfvén times. The sonic toroidal flow has greatly reduced the rate at which thermal energy is lost when  $\beta=2\%$ . But energy is still transported out to the wall, unlike the case when  $\beta=1\%$  where a sonic toroidal flow maintains confinement.

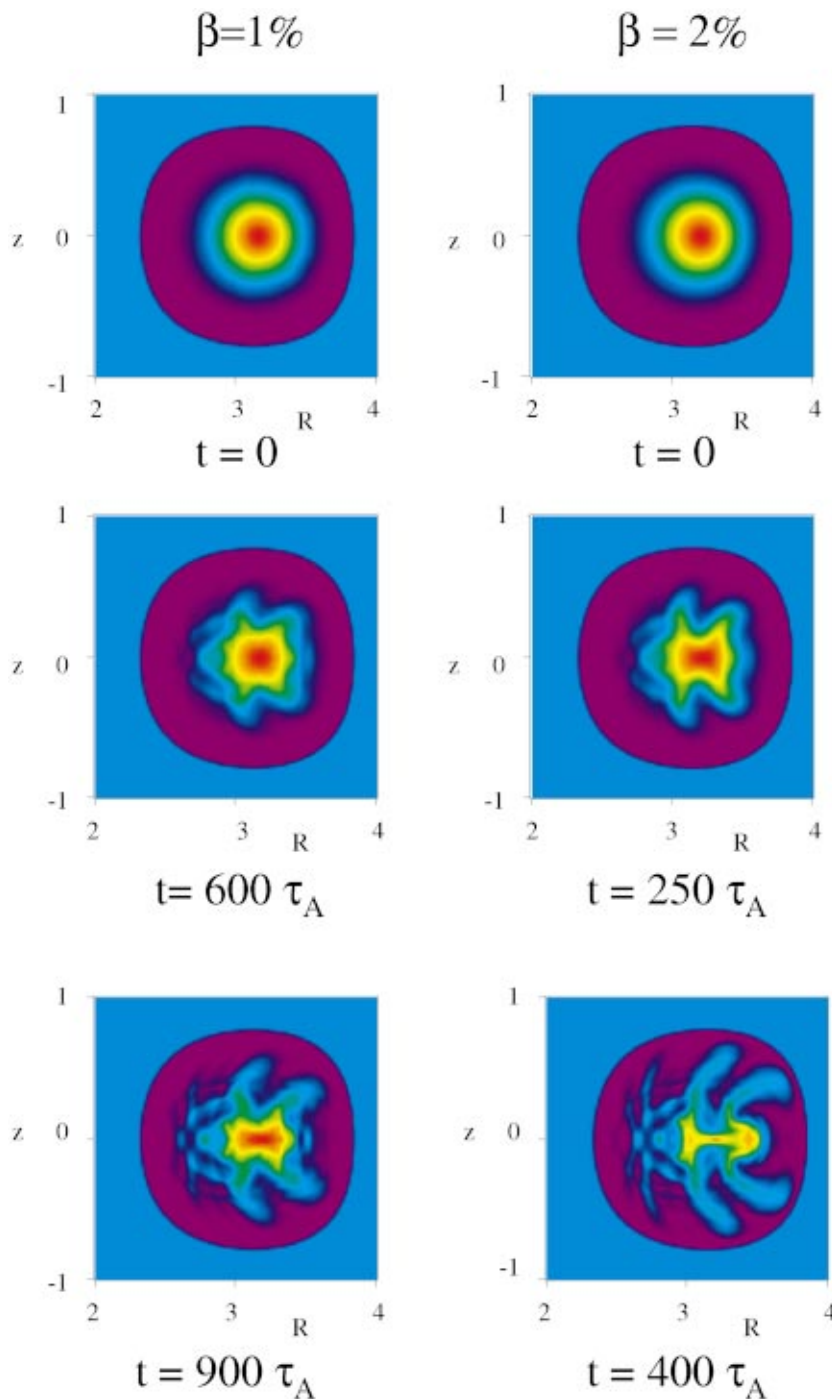


FIG. 2. (Color) Disruptions at high  $\beta$ . The series of plots shows the nonlinear evolution of the temperature in the poloidal plane ( $R, z$ ) at toroidal angle  $\phi = 0$ , for a flow-free tokamak plasma with  $\beta = 1\%$  (left-hand side) and  $\beta = 2\%$  (right-hand side). The hottest plasma is located in the red region. The plasma becomes progressively cooler through the orange, yellow, green, and blue regions, with the coldest plasma located in the violet region. The boundary of the plasma lies at the inner edge of the light blue area located at the edge of each plot.

### C. Transport coefficients

The transport coefficients used in these simulations are much larger than those at the center of a large, hot tokamak where the Lundquist number  $S \sim 10^8 - 10^9$ . The plots on the right-hand side of Fig. 4 show the effect of a reduction in the magnitude of the transport coefficients on the nonlinear stability of high  $\beta$  tokamaks with toroidal flows. The simulation on the right-hand side of Fig. 4 is identical to that on the left-hand side except that the magnitude of the transport coefficients for the simulation on the right has been reduced by a factor of 30. The spiralling transport of thermal energy to the wall seen when  $\eta = \mu = D = 3 \times 10^{-4}$  ( $S = 3.3 \times 10^3$ ) is

eliminated when the transport coefficients are reduced in magnitude to  $\eta = \mu = D = 1 \times 10^{-5}$  ( $S = 1 \times 10^5$ ), and stable confinement is maintained.

We have also carried out a simulation identical to that shown on the left-hand side of Fig. 3 where  $\beta = 1\%$  and the Mach number  $M = 0.3$ , except that the transport coefficients have been reduced in magnitude by a factor of 10 to  $\eta = \mu = D = 3 \times 10^{-5}$ . Again, the spiralling transport of thermal energy to the wall is eliminated when the transport coefficients are reduced, and confinement is maintained.

However, when the temperature is increased to  $\beta = 6\%$  with  $\eta = \mu = D = 1 \times 10^{-5}$ , a sound speed toroidal flow is no

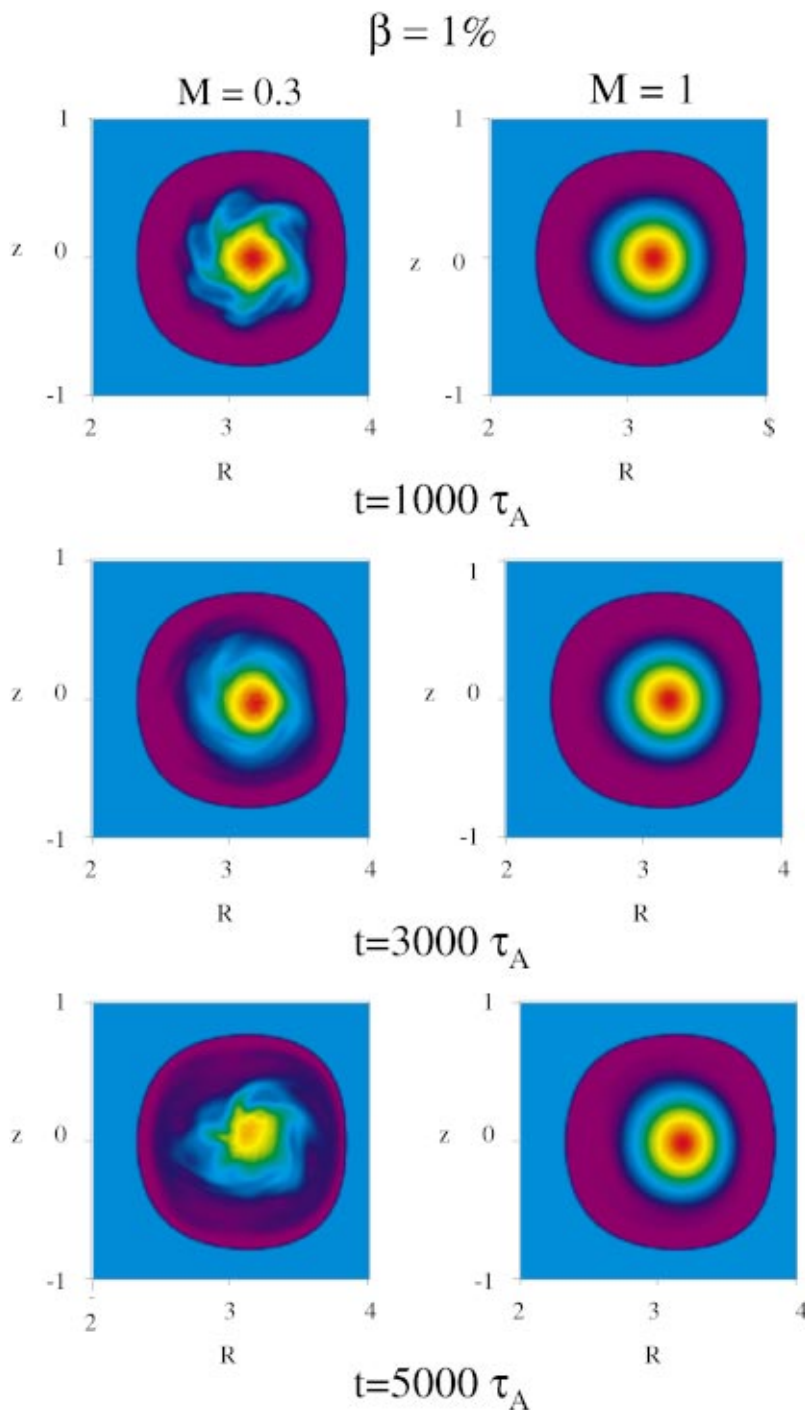


FIG. 3. (Color) Nonlinear stability with toroidal flows. The series of plots shows the nonlinear evolution of the temperature in the poloidal plane ( $R, z$ ) at toroidal angle  $\phi=0$ , for a  $\beta=1\%$  tokamak plasma with a toroidal flow of Mach number  $M=0.3$  (left-hand side) and  $M=1$  (right-hand side).

longer sufficient to maintain confinement. Confinement is lost as thermal energy is rapidly convected to the wall in a couple of hundred Alfvén times. A toroidal flow of Mach number  $M$  becomes less effective at stabilizing a plasma as  $\beta$  is increased.

## V. DISCUSSION

Our numerical simulations demonstrate that disruptive high  $\beta$  tokamaks can be stabilized by the addition of a sheared toroidal flow. In flow-free tokamaks, confinement is rapidly destroyed by fingers of hot plasma that balloon out from the center of the discharge to the wall at large  $R$ . The

addition of a subsonic toroidal flow acts to stabilize the plasma. The fingers still grow, but much more slowly. Instead of ballooning out to the wall at large  $R$ , the fingers are more uniform in poloidal angle and rotate about the magnetic axis. Rather than a rapid, direct loss of confinement, thermal energy spirals to the wall. With further increases in the magnitude of the toroidal flow speed, the fingers are eliminated altogether and confinement is maintained. As the transport coefficients are reduced in magnitude, the stabilizing effect of the toroidal flow becomes even stronger. When the magnitude of the transport coefficients are reduced in a flow-free plasma, the fingers generated become more numerous and

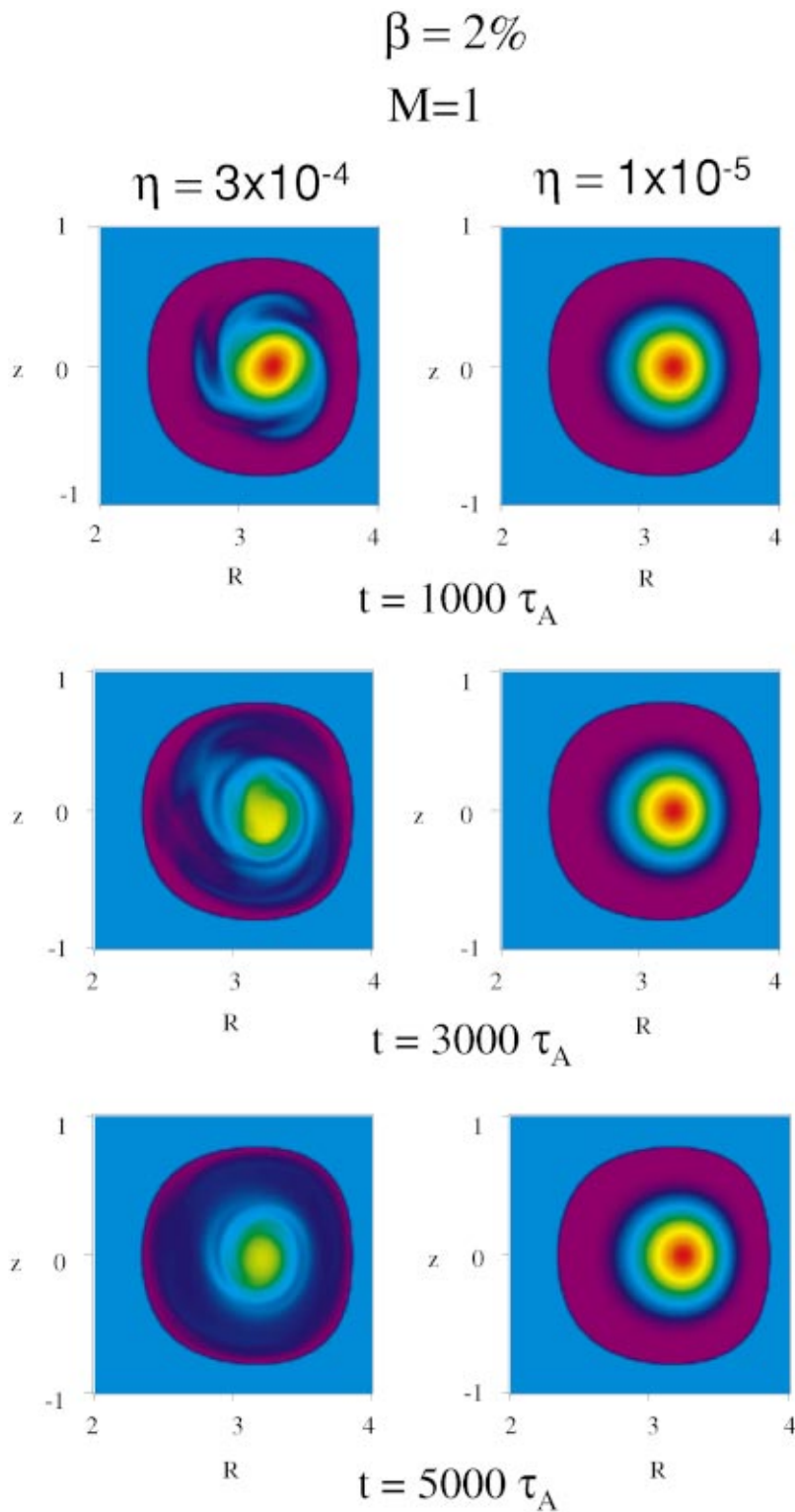


FIG. 4. (Color) Transport coefficients. The series of plots shows the nonlinear evolution of the temperature in the poloidal plane ( $R, z$ ) at toroidal angle  $\phi=0$ , for a  $\beta=2\%$  tokamak plasma with a sonic toroidal flow ( $M=1$ ). The classical transport coefficients  $\eta=\mu=D=3 \times 10^{-4}$  for the plots on the left-hand side while  $\eta=\mu=D=1 \times 10^{-5}$  for the plots on the right-hand side.

narrower in width.<sup>4</sup> But these narrower fingers at smaller  $\eta$  and  $\mu$  destroy confinement at the same rate as the wider fingers at larger  $\eta$  and  $\mu$ .<sup>4</sup> The loss of confinement in flow-free tokamak plasmas is independent of the magnitude of the Lundquist number  $S$ . However, the stabilizing effect of the toroidal flow increases as  $S$  becomes larger. The toroidal flow is more effective at shearing apart and stabilizing the narrower structures at larger  $S$ .

In the ideal MHD approximation, the transport coefficients are neglected and the growth rate of ballooning modes at large  $\beta$  is proportional to the sound speed or, equivalently, the square root of the temperature.<sup>12</sup> But the structure of the fingers generated in our nonlinear simulations depends on the magnitude of the resistivity  $\eta$ .<sup>4</sup> As the magnitude of the resistivity decreases, the number  $N$  of fingers generated increases as  $N \sim \eta^{-1/2}$  while the width  $w$  of each finger de-

creases as  $w \sim \eta^{1/2}$ . The resistivity  $\eta$  remains important, and cannot be neglected, even as  $\eta \rightarrow 0$ . Although the rate at which the fingers grow is indeed independent of the magnitude of  $\eta$ , the growth rate does not scale with  $\beta$  as the ideal MHD ballooning mode growth rate  $\beta^{1/2}$ . When the magnitude of temperature in the simulations is doubled, the growth rate of the fingers is approximately doubled (Fig. 2). The growth of the fingers is therefore roughly proportional to  $\beta$ . At somewhat lower, although still large, values of  $\beta$ , an otherwise disruptive plasma can be stabilized by a sound speed toroidal flow. However, as  $\beta$  increases the magnitude of a sound speed toroidal flow increases only as  $\beta^{1/2}$ . For very large  $\beta$ , the fingers grow too rapidly to be suppressed by a sound speed flow. But a sound speed toroidal flow increases the critical value of  $\beta$  below which confinement is maintained without disruptions.

## ACKNOWLEDGMENT

This research was supported by the U.S. Department of Energy.

- <sup>1</sup>E. D. Fredrickson, K. McGuire, Z. Chang, A. Janos, M. Bell, R. V. Budny, C. E. Bush, J. Manickam, H. Mynick, R. Nazikian, and G. Taylor, *Phys. Plasmas* **2**, 4216 (1995).
- <sup>2</sup>R. G. Kleva and P. N. Guzdar, *Phys. Rev. Lett.* **80**, 3081 (1998).
- <sup>3</sup>R. G. Kleva and P. N. Guzdar, *Phys. Plasmas* **7**, 1163 (2000).
- <sup>4</sup>R. G. Kleva and P. N. Guzdar, *Phys. Plasmas* **8**, 103 (2001).
- <sup>5</sup>W. A. Cooper, *Plasma Phys. Controlled Fusion* **30**, 1805 (1988).
- <sup>6</sup>K. Grassie and M. Krech, *Phys. Fluids B* **2**, 1864 (1990).
- <sup>7</sup>F. L. Waelbroeck and L. Chen, *Phys. Fluids B* **3**, 601 (1991).
- <sup>8</sup>R. L. Miller, F. L. Waelbroeck, A. B. Hassam, and R. E. Waltz, *Phys. Plasmas* **2**, 3676 (1995).
- <sup>9</sup>R. G. Kleva and P. N. Guzdar, *Phys. Plasmas* **6**, 116 (1999).
- <sup>10</sup>S. T. Zalesak, *J. Comput. Phys.* **40**, 497 (1981).
- <sup>11</sup>Y. Kuribara, *Mon. Weather Rev.* **93**, 13 (1965).
- <sup>12</sup>D. Biskamp, *Nonlinear Magnetohydrodynamics* (Cambridge University Press, Cambridge, UK, 1993), p. 69.